Number 3 Volume 13 September2006 Journal of Engineering

ANALYSIS OF CONTINUOUS COMPOSITE CONCRETE-STEEL GIRDERS WITH PARTIAL INTERACTION

Dr. Husain M. Husain Qusay Asa'ad Al-Aquly Dr. Mohannad H. Al-Sherrawi
Dept. of Civil Engineering, University of Baghdad, Iraq

ABSTRACT

In the present study, a general nonlinear one-dimensional finite element beam model is developed for the analysis of composite beams. The proposed model is based on the partial interaction theory of composite beams where the flexibility of shear connectors is allowed. By using a layered approach for the composite beam cross-section and including the material nonlinear behavior of concrete, steel, shear connector and reinforcing steel, the proposed method of analysis is capable of predicting the response of composite beams throughout the elastic, inelastic and ultimate load ranges in one complete analysis.

Numerical case studies are presented to demonstrate the validity and applicability of the present method. The results are compared with experimental and analytical or numerical results obtained by other investigators. Also the results are compared with ANSYS package results. The maximum differences in deflection and slip for the examples considered are 12% and 14% respectively when compared with ANSYS and 5% and 11% when compared with experimental work. Accordingly, the proposed nonlinear finite element model represents an efficient and simple tool for the full range analysis of composite beams.

الخلاصة

في هذه الدراسة تم عرض نموذج عام لا خطي ذي بعد واحد بطريقة العناصر المحددة لدراسة العتبات المركبة. والنموذج المقترح مبني على أساس نظرية الربط الجزئي للعتبات المركبة إذ أن مرونة روابط القص شئ مسموح به. إن الطريقة المقترحة قادرة على أن تعطي تصوراً واضحاً عن تصرف العتبات المركبة خلال التحمل الخطي واللاخطي والحمل الأعظم في تحليل واحد وذلك باستعمال طريقة تجزئة المقطع للعتبة إلى طبقات بالإضافة إلى التصرف اللاخطي لمادة الخرسانة والحديد وروابط القص وحديد التسليح.

ولاختبار صحة ودقة الطريقة المقترحة، تم تطبيقها على دراسات سابقة حيث تمت المقارنة مع النتائج التجريبية والتحليلية المستخلصة من قبل باحثين سابقين و كذلك تمت المقارنة مع البرنامج الجاهز ANSYS . إن القيم العظمى للفرو قات في الهطول و الانزلاق للأمثلة التي تم اعتمادها في هذه الدراسة كانت 12% و 14% على التوالي عند مقارنتها مع برنامج (ANSYS) و5% و 11% عند مقارنتها مع الفحوصات العملية. وبناء على ما تقدم، فإن النموذج المقترح نموذج فعال كما أنه بسيط للتحليل الكامل للعتبات المركبة ويمكن استعماله للتصميم والتحليل الاعتياديين.

KEYWORDS

Composite beams, finite element, nonlinear analysis, shear-slip, shear connector.

INTRODUCTION

A composite beam is an assemblage of different materials so as to form a single unit in order to exploit the prominent quality of these materials according to their position within the cross-section of the beam, Fig.(1).

In this work, a new composite beam element for the analysis of steel-concrete girders with partial composite action is developed. Computer programs are developed using FORTRAN

language. The programs take into account the slip, uplift (vertical separation), haunched slab, unsymmetrical I-cross section for steel beams and the applied load position (whether it is applied on the concrete slab or on the steel beam).

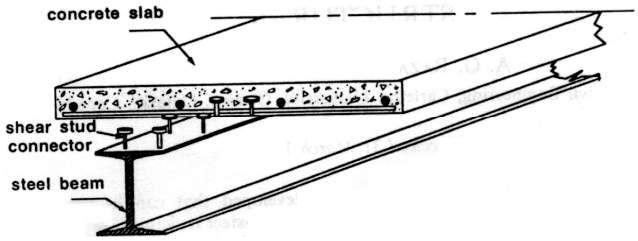

Fig. (1) Typical portion of a composite beam.

The horizontal displacements in steel beam u_{st}, concrete slab u_c, and slab reinforcement u_{rs}, are (Fig. (2)):

$$u_{st} = u_{0st} - z_{st}\frac{dw_{st}}{dx} \quad ; \quad u_c = u_{0c} - z_c\frac{dw_c}{dx} \quad ; \quad u_{rs} = u_{0c} - d_o\frac{dw_c}{dx} \tag{1}$$

where

$w_{st}(x)$ and $w_c(x)$ the vertical displacements for the steel beam and the concrete slab, respectively.

$u_{0st}(x)$ and $u_{0c}(x)$: the axial displacements of the steel beam and of the concrete slab respectively at their reference axes. It is to be noted that it is customary to select the geometric centroid of the corresponding component as the reference point, but any other point can be used as well.

$\frac{dw_{st}}{dx}$ and $\frac{dw_c}{dx}$: the slopes of the deflection curve in the steel beam and the concrete slab, respectively.

The relative displacements between the concrete and the steel components along their interface are:

The slip, u_{cs}, between the concrete slab and the steel beam is given as the difference in the displacements between the bottom surface of the concrete slab and the top surface of the steel beam in the longitudinal direction (positive to the right side), i.e.:

$$u_{cs} = u_c(z_c = -y_c) - u_{st}(z_{st} = y_{st}) = u_{0c} - u_{0s} + y_{st}\frac{dw_s}{dx} + y_c\frac{dw_c}{dx} \tag{2}$$

The separation (uplift), w_{sc}, in the vertical direction between the concrete slab and the steel beam is the difference in deflections between the steel beam and the concrete slab at the point under consideration. It may be expressed as:

$$w_{sc} = w_{st} - w_c \tag{3}$$

where

y_{st} and y_c: the distances from the reference points to the interface of the steel and concrete components, respectively.

The corresponding section deformations (non-zero strains):

$$\varepsilon_{st} = \frac{du_{0st}}{dx} - z_{st}\frac{d^2w_{st}}{dx^2} = \varepsilon_{0st} - z_{st}\frac{d^2w_{st}}{dx^2} \quad ; \quad \varepsilon_c = \frac{du_{0c}}{dx} - z_c\frac{d^2w_c}{dx^2} = \varepsilon_{0c} - z_c\frac{d^2w_c}{dx^2} \quad ;$$

$$\varepsilon_{rs} = \frac{du_{0c}}{dx} - d_o \frac{d^2 w_c}{dx^2} = \varepsilon_{0c} - d_o \frac{d^2 w_c}{dx^2} \quad (4)$$

where

ε_{0st} and ε_{0c} are the axial strains at the reference axes of the steel and the concrete sections, respectively.

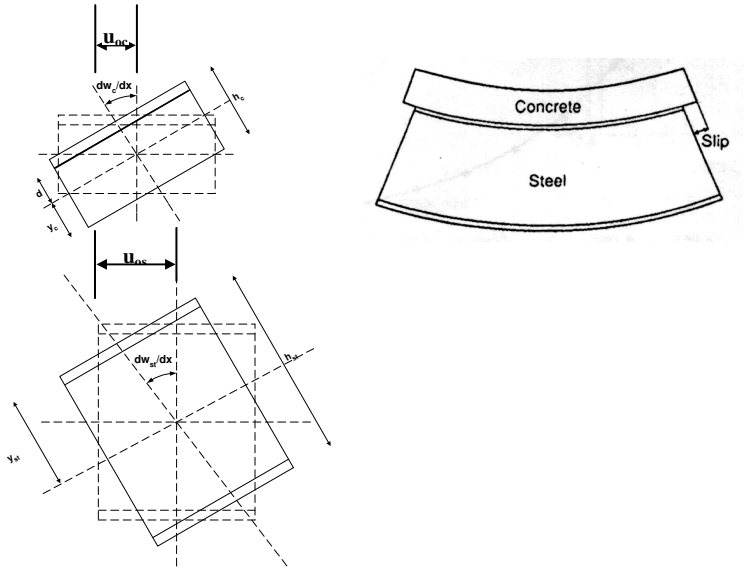

Fig. (2) Deformations of composite beam segment.

The slip strain in the shear-connecting layer is indirectly given as the longitudinal (or normal) strain differences between the bottom surface of the concrete slab and the top surface of the steel beam.

The stresses in the longitudinal direction can be obtained by using the corresponding constitutive relationships given in later or in general:

$$\sigma_{st} = f_{st}(\varepsilon_{st}) \quad (5)$$

$$\sigma_c = f_c(\varepsilon_c) \quad (6)$$

$$\sigma_{rs} = f_{rs}(\varepsilon_{rs}) \quad (7)$$

and for the shear connector layer:

$$q = f_{slip}(u_{cs}) \quad (8)$$

$$F_n = f_{separation}(w_{sc}) \quad (9)$$

The resulting forces given as the bending moments (with respect to the centerline of the steel section) and the axial forces in the components are thus,

$$M_{st} = \int_{As} \sigma_{st} z_{st} dA \quad (10)$$

$$M_c = \int_{Ac} \sigma_c [z_c + y_{st} + y_c] dA \quad (11)$$

$$M_{rs} = \int_{Ars} \sigma_{rs} [d + y_{st} + y_c] dA \quad (12)$$

and

$$F_{st} = \int_{As} \sigma_{st} dA \tag{13}$$

$$F_c = \int_{Ac} \sigma_c dA \tag{14}$$

$$F_{rs} = \int_{Ars} \sigma_{rs} dA \tag{15}$$

Since the beam is not subjected to any axial force, then:

$$F_{st} + F_c + F_{rs} = 0 \tag{16}$$

and the resultant moment on the composite section:

$$M_T = M_{st} + M_c + M_{rs} \tag{17}$$

COMPOSITE BEAM ELEMENT DESCRIPTION

A composite beam element is composed of elements of steel beam, concrete slab and shear connectors as shown in Fig. (3). It has two coordinate systems, X_{st} and Z_{st} for the steel part and X_c and Z_c for the concrete part. The Z-axis coincides with the vertical axis of symmetry of the cross section. The composite element is also divided into a discrete number of concrete and steel layers as shown in Fig. (4). This layering will be discussed later.

A three-node (one-dimensional) composite beam element with fourteen degrees of freedom is developed. The element is equipped with six degrees of freedom for each end node of the element and two horizontal degrees of freedom are used also at mid-length node of the element to improve its axial behavior (Al-Aquly, 2002).

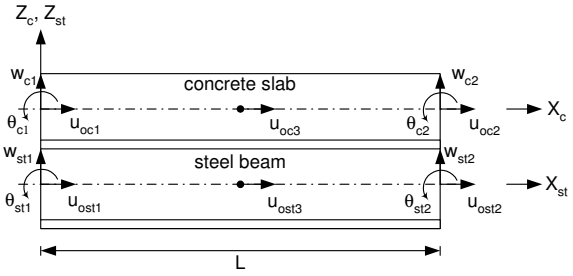

Fig. (3) Composite beam element with displacement components (rigid body modes).

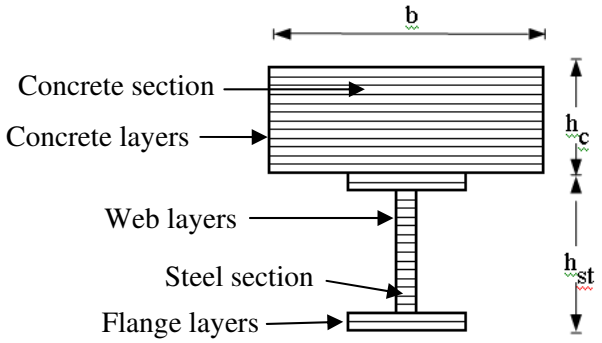

Fig. (4): Layered beam section.

Element Displacements

Vectors that represent the axial and bending displacements are {u} and {b}, respectively.

$$\{u\} = [u_{0st1} \quad u_{0c1} \quad u_{0st2} \quad u_{0c2} \quad u_{0st3} \quad u_{0c3}]^T \tag{18}$$

$$\{b\} = [w_{st1} \quad \theta_{st1} \quad w_{c1} \quad \theta_{c1} \quad w_{st2} \quad \theta_{st2} \quad w_{c2} \quad \theta_{c2}]^T \tag{19}$$

where, $\theta_{st} = \frac{dw_{st}}{dx}$ and $\theta_c = \frac{dw_c}{dx}$: the slopes of the steel and concrete components.

These displacement components can be assembled in one column vector {e}:

$$\{e\} = \begin{Bmatrix} u \\ b \end{Bmatrix} = [u_{0st1}\ u_{0c1}\ w_{st1}\ \theta_{st1}\ w_{c1}\ \theta_{c1}\ u_{0st2}\ u_{0c2}\ w_{st2}\ \theta_{st2}\ w_{c2}\ \theta_{c2}\ u_{0st3}\ u_{0c3}]^T \tag{20}$$

To approximate the displacements of the composite beam, cubic Hermitian polynomials are employed for the transverse deflection and quadratic functions are used for the axial displacements. The quadratic axial displacements are achieved by introducing an extra node in the middle of the element with two axial degrees of freedom, one in each beam component.

Evaluation of the Tangent Stiffness Matrix

The tangent stiffness matrix is generated at the mid-length of the composite beam element and it is assumed to be constant along the element for the nonlinear behavior. The tangent stiffness matrix of a composite beam element, is given by:

$$[k_T] = \int_{vol} [B]^T [\bar{E}][B] dvol \quad (21)$$

The final finite element equation may be symbolically written as:

$$\{F\} = ([k_0] + [k_{slip}] + [k_{uplift}])\{e\} \quad (22)$$

where

$[k_o]$: the stiffness matrix of the composite beam without shear interaction, and

$[k_{slip}]$ and $[k_{uplift}]$: shear connector contribution to the beam stiffness.

Finally, the contribution of the composite beam components can be expressed as:

$$[k^e] = [k^e]_{st} + [k^e]_c + [k^e]_{rs} + [k^e]_{cs} + [k^e]_{sc} \quad (23)$$

where

$[k^e]_{st}$, $[k^e]_c$, $[k^e]_{rs}$, $[k^e]_{cs}$, and $[k^e]_{sc}$: steel beam, concrete slab, tangential shear connector layer, and transverse shear connector layer element stiffness matrix.

These matrices are derived for the purpose of this study and they are given as:

$$[k^e]_{st} = E_{st} \begin{bmatrix}
\frac{7A_{st}}{3L} & 0 & 0 & 0 & 0 & 0 & \frac{A_{st}}{3L} & 0 & 0 & 0 & 0 & 0 & \frac{-8A_{st}}{3L} & 0 \\
0 & 0 & 0 & 0 & 0 & 0 & 0 & 0 & 0 & 0 & 0 & 0 & 0 & 0 \\
0 & 0 & \frac{12I_{ts}}{L^3} & \frac{6I_{st}}{L^2} & 0 & 0 & 0 & 0 & \frac{-12I_{st}}{L^3} & \frac{6I_{st}}{L^2} & 0 & 0 & 0 & 0 \\
0 & 0 & \frac{6I_{ts}}{L^2} & \frac{4I_{st}}{L} & 0 & 0 & 0 & 0 & \frac{-6I_{st}}{L^2} & \frac{2I_{st}}{L} & 0 & 0 & 0 & 0 \\
0 & 0 & 0 & 0 & 0 & 0 & 0 & 0 & 0 & 0 & 0 & 0 & 0 & 0 \\
0 & 0 & 0 & 0 & 0 & 0 & 0 & 0 & 0 & 0 & 0 & 0 & 0 & 0 \\
\frac{A_{st}}{3L} & 0 & 0 & 0 & 0 & 0 & \frac{7A_{st}}{3L} & 0 & 0 & 0 & 0 & 0 & \frac{-8A_{st}}{3L} & 0 \\
0 & 0 & 0 & 0 & 0 & 0 & 0 & 0 & 0 & 0 & 0 & 0 & 0 & 0 \\
0 & 0 & \frac{-12I_{ts}}{L^3} & \frac{-6I_{st}}{L^2} & 0 & 0 & 0 & 0 & \frac{12I_{st}}{L^3} & \frac{-6I_{st}}{L^2} & 0 & 0 & 0 & 0 \\
0 & 0 & \frac{6I_{ts}}{L^2} & \frac{2I_{st}}{L} & 0 & 0 & 0 & 0 & \frac{-6I_{st}}{L^2} & \frac{4I_{st}}{L} & 0 & 0 & 0 & 0 \\
0 & 0 & 0 & 0 & 0 & 0 & 0 & 0 & 0 & 0 & 0 & 0 & 0 & 0 \\
0 & 0 & 0 & 0 & 0 & 0 & 0 & 0 & 0 & 0 & 0 & 0 & 0 & 0 \\
\frac{-8A_{ts}}{3L} & 0 & 0 & 0 & 0 & 0 & \frac{-8A_{st}}{3L} & 0 & 0 & 0 & 0 & 0 & \frac{16A_{st}}{3L} & 0 \\
0 & 0 & 0 & 0 & 0 & 0 & 0 & 0 & 0 & 0 & 0 & 0 & 0 & 0
\end{bmatrix} \quad (24)$$

$$[k^e]_c = E_c \begin{bmatrix}
0 & 0 & 0 & 0 & 0 & 0 & 0 & 0 & 0 & 0 & 0 & 0 & 0 & 0 \\
0 & \frac{7A_c}{3L} & 0 & 0 & 0 & 0 & 0 & \frac{A_c}{3L} & 0 & 0 & 0 & 0 & 0 & \frac{-8A_c}{3L} \\
0 & 0 & 0 & 0 & 0 & 0 & 0 & 0 & 0 & 0 & 0 & 0 & 0 & 0 \\
0 & 0 & 0 & 0 & 0 & 0 & 0 & 0 & 0 & 0 & 0 & 0 & 0 & 0 \\
0 & 0 & 0 & 0 & \frac{12I_c}{L^3} & \frac{6I_c}{L^2} & 0 & 0 & 0 & 0 & \frac{-12I_c}{L^3} & \frac{6I_c}{L^2} & 0 & 0 \\
0 & 0 & 0 & 0 & \frac{6I_c}{L^2} & \frac{4I_c}{L} & 0 & 0 & 0 & 0 & \frac{-6I_c}{L^2} & \frac{2I_c}{L} & 0 & 0 \\
0 & 0 & 0 & 0 & 0 & 0 & 0 & 0 & 0 & 0 & 0 & 0 & 0 & 0 \\
0 & \frac{A_c}{3L} & 0 & 0 & 0 & 0 & 0 & \frac{7A_c}{3L} & 0 & 0 & 0 & 0 & 0 & \frac{-8A_c}{3L} \\
0 & 0 & 0 & 0 & 0 & 0 & 0 & 0 & 0 & 0 & 0 & 0 & 0 & 0 \\
0 & 0 & 0 & 0 & 0 & 0 & 0 & 0 & 0 & 0 & 0 & 0 & 0 & 0 \\
0 & 0 & 0 & 0 & \frac{-12I_c}{L^3} & \frac{-6I_c}{L^2} & 0 & 0 & 0 & 0 & \frac{12I_c}{L^3} & \frac{-6I_c}{L^2} & 0 & 0 \\
0 & 0 & 0 & 0 & \frac{6I_c}{L^2} & \frac{2I_c}{L} & 0 & 0 & 0 & 0 & \frac{-6I_c}{L^2} & \frac{4I_c}{L} & 0 & 0 \\
0 & 0 & 0 & 0 & 0 & 0 & 0 & 0 & 0 & 0 & 0 & 0 & 0 & 0 \\
0 & \frac{-8A_c}{3L} & 0 & 0 & 0 & 0 & 0 & \frac{-8A_c}{3L} & 0 & 0 & 0 & 0 & 0 & \frac{16A_c}{3L}
\end{bmatrix} \tag{25}$$

$$[k^e]_{rs} = E_{rs}A_{rs} \begin{bmatrix}
0 & 0 & 0 & 0 & 0 & 0 & 0 & 0 & 0 & 0 & 0 & 0 & 0 & 0 \\
0 & \frac{7}{3L} & 0 & 0 & 0 & \frac{-3d}{L} & 0 & \frac{1}{3L} & 0 & 0 & 0 & \frac{-d}{L} & 0 & \frac{-8}{3L} \\
0 & 0 & 0 & 0 & 0 & 0 & 0 & 0 & 0 & 0 & 0 & 0 & 0 & 0 \\
0 & 0 & 0 & 0 & 0 & 0 & 0 & 0 & 0 & 0 & 0 & 0 & 0 & 0 \\
0 & 0 & 0 & 0 & \frac{12d^2}{L^3} & \frac{6d^2}{L^2} & 0 & 0 & 0 & 0 & \frac{-12d^2}{L^3} & \frac{6d^2}{L^2} & 0 & 0 \\
0 & \frac{-3d}{L} & 0 & 0 & \frac{6d^2}{L^2} & \frac{4d^2}{L} & 0 & \frac{-d}{L} & 0 & 0 & \frac{-6d^2}{L^2} & \frac{2d^2}{L} & 0 & \frac{4d}{L} \\
0 & 0 & 0 & 0 & 0 & 0 & 0 & 0 & 0 & 0 & 0 & 0 & 0 & 0 \\
0 & \frac{1}{3L} & 0 & 0 & 0 & \frac{-d}{L} & 0 & \frac{7}{3L} & 0 & 0 & 0 & \frac{-3d}{L} & 0 & \frac{-8}{3L} \\
0 & 0 & 0 & 0 & 0 & 0 & 0 & 0 & 0 & 0 & 0 & 0 & 0 & 0 \\
0 & 0 & 0 & 0 & 0 & 0 & 0 & 0 & 0 & 0 & 0 & 0 & 0 & 0 \\
0 & 0 & 0 & 0 & \frac{-12d^2}{L^3} & \frac{-6d^2}{L^2} & 0 & 0 & 0 & 0 & \frac{12d^2}{L^3} & \frac{-6d^2}{L^2} & 0 & 0 \\
0 & \frac{-d}{L} & 0 & 0 & \frac{6d^2}{L^2} & \frac{2d^2}{L} & 0 & \frac{-3d}{L} & 0 & 0 & \frac{-6d^2}{L^2} & \frac{4d^2}{L} & 0 & \frac{4d}{L} \\
0 & 0 & 0 & 0 & 0 & 0 & 0 & 0 & 0 & 0 & 0 & 0 & 0 & 0 \\
0 & \frac{-8}{3L} & 0 & 0 & 0 & \frac{4d}{L} & 0 & \frac{-8}{3L} & 0 & 0 & 0 & \frac{4d}{L} & 0 & \frac{16}{3L}
\end{bmatrix} \tag{26}$$

$$[k^e]_{cs} = K_s \begin{bmatrix}
\frac{2L}{15} & \frac{-2L}{15} & \frac{y_{st}}{10} & \frac{-7Ly_{st}}{60} & \frac{y_c}{10} & \frac{-7Ly_c}{60} & \frac{-L}{30} & \frac{L}{30} & \frac{-y_{st}}{10} & \frac{Ly_{st}}{20} & \frac{-y_c}{10} & \frac{Ly_c}{20} & \frac{L}{15} & \frac{-L}{15} \\
\frac{-2L}{15} & \frac{2L}{15} & \frac{-y_{st}}{10} & \frac{7Ly_{st}}{60} & \frac{-y_c}{10} & \frac{7Ly_c}{60} & \frac{L}{30} & \frac{-L}{30} & \frac{y_{st}}{10} & \frac{-Ly_{st}}{20} & \frac{y_c}{10} & \frac{-Ly_c}{20} & \frac{-L}{15} & \frac{L}{15} \\
\frac{y_{st}}{10} & \frac{-y_{st}}{10} & \frac{6y_{st}^2}{5L} & \frac{y_{st}^2}{10} & \frac{6y_{st}y_c}{5L} & \frac{y_{st}y_c}{10} & \frac{y_{st}}{10} & \frac{-y_{st}}{10} & \frac{-6y_{st}^2}{5L} & \frac{y_{st}^2}{10} & \frac{-6y_{st}y_c}{5L} & \frac{y_{st}y_c}{10} & \frac{4y_{st}}{5} & \frac{-4y_{st}}{5} \\
\frac{-7Ly_{st}}{60} & \frac{7Ly_{st}}{60} & \frac{y_{st}^2}{10} & \frac{2Ly_{st}^2}{15} & \frac{y_{st}y_c}{10} & \frac{2y_{st}y_cL}{15} & \frac{Ly_{st}}{20} & \frac{-Ly_{st}}{20} & \frac{-y_{st}^2}{10} & \frac{-Ly_{st}^2}{30} & \frac{-y_{st}y_c}{10} & \frac{-Ly_{st}y_c}{30} & \frac{Ly_{st}}{15} & \frac{-Ly_{st}}{15} \\
\frac{y_c}{10} & \frac{-y_c}{10} & \frac{6y_{st}y_c}{5L} & \frac{y_{st}y_c}{10} & \frac{6y_c^2}{5L} & \frac{y_c^2}{10} & \frac{y_c}{10} & \frac{-y_c}{10} & \frac{-6y_{st}y_c}{5L} & \frac{y_{st}y_c}{10} & \frac{-6y_c^2}{5L} & \frac{y_c^2}{10} & \frac{4y_c}{5} & \frac{-4y_c}{5} \\
\frac{-7Ly_c}{60} & \frac{7Ly_c}{60} & \frac{y_{st}y_c}{10} & \frac{2y_{st}y_cL}{15} & \frac{y_c^2}{10} & \frac{2Ly_c^2}{15} & \frac{Ly_c}{20} & \frac{-Ly_c}{20} & \frac{-y_{st}y_c}{10} & \frac{-Ly_{st}y_c}{30} & \frac{-y_c^2}{10} & \frac{-Ly_c^2}{30} & \frac{Ly_c}{15} & \frac{-Ly_c}{15} \\
\frac{-L}{30} & \frac{L}{30} & \frac{y_{st}}{10} & \frac{Ly_{st}}{20} & \frac{y_c}{10} & \frac{Ly_c}{20} & \frac{2L}{15} & \frac{-2L}{15} & \frac{-y_{st}}{10} & \frac{-7Ly_{st}}{60} & \frac{-y_c}{10} & \frac{-7Ly_c}{60} & \frac{L}{15} & \frac{-L}{15} \\
\frac{L}{30} & \frac{-L}{30} & \frac{-y_{st}}{10} & \frac{-Ly_{st}}{20} & \frac{-y_c}{10} & \frac{-Ly_c}{20} & \frac{-2L}{15} & \frac{2L}{15} & \frac{y_{st}}{10} & \frac{7Ly_{st}}{60} & \frac{y_c}{10} & \frac{7Ly_c}{60} & \frac{-L}{15} & \frac{L}{15} \\
\frac{-y_{st}}{10} & \frac{y_{st}}{10} & \frac{-6y_{st}^2}{5L} & \frac{-y_{st}^2}{10} & \frac{-6y_{st}y_c}{5L} & \frac{-y_{st}y_c}{10} & \frac{-y_{st}}{10} & \frac{y_{st}}{10} & \frac{6y_{st}^2}{5L} & \frac{-y_{st}^2}{10} & \frac{6y_{st}y_c}{5L} & \frac{-y_{st}y_c}{10} & \frac{-4y_{st}}{5} & \frac{4y_{st}}{5} \\
\frac{Ly_{st}}{20} & \frac{-Ly_{st}}{20} & \frac{y_{st}^2}{10} & \frac{-Ly_{st}^2}{30} & \frac{y_{st}y_c}{10} & \frac{-Ly_{st}y_c}{30} & \frac{-7Ly_{st}}{60} & \frac{7Ly_{st}}{60} & \frac{-y_{st}^2}{10} & \frac{2Ly_{st}^2}{15} & \frac{-y_{st}y_c}{10} & \frac{2Ly_{st}y_c}{15} & \frac{Ly_{st}}{15} & \frac{-Ly_{st}}{15} \\
\frac{-y_c}{10} & \frac{y_c}{10} & \frac{-6y_{st}y_c}{5L} & \frac{-y_{st}y_c}{10} & \frac{-6y_c^2}{5L} & \frac{-y_c^2}{10} & \frac{-y_c}{10} & \frac{y_c}{10} & \frac{6y_{st}y_c}{5L} & \frac{-y_{st}y_c}{10} & \frac{6y_c^2}{5L} & \frac{-y_c^2}{10} & \frac{-4y_c}{5} & \frac{4y_c}{5} \\
\frac{Ly_c}{20} & \frac{-Ly_c}{20} & \frac{y_{st}y_c}{10} & \frac{-Ly_{st}y_c}{30} & \frac{y_c^2}{10} & \frac{-Ly_c^2}{30} & \frac{-7Ly_c}{60} & \frac{7Ly_c}{60} & \frac{-y_{st}y_c}{10} & \frac{2Ly_{st}y_c}{15} & \frac{-y_c^2}{10} & \frac{2Ly_c^2}{15} & \frac{Ly_c}{15} & \frac{-Ly_c}{15} \\
\frac{L}{15} & \frac{-L}{15} & \frac{4y_{st}}{5} & \frac{Ly_{st}}{15} & \frac{4y_c}{5} & \frac{Ly_c}{15} & \frac{-L}{15} & \frac{L}{15} & \frac{-4y_{st}}{5} & \frac{Ly_{st}}{15} & \frac{-4y_c}{5} & \frac{Ly_c}{15} & \frac{8L}{15} & \frac{-8L}{15} \\
\frac{-L}{15} & \frac{L}{15} & \frac{-4y_{st}}{5} & \frac{-Ly_{st}}{15} & \frac{-4y_c}{5} & \frac{-Ly_c}{15} & \frac{-L}{15} & \frac{L}{15} & \frac{4y_{st}}{5} & \frac{-Ly_{st}}{15} & \frac{4y_c}{5} & \frac{-Ly_c}{15} & \frac{-8L}{15} & \frac{8L}{15}
\end{bmatrix} \tag{27}$$

$$[k^e]_{sc} = K_n \begin{bmatrix}
0 & 0 & 0 & 0 & 0 & 0 & 0 & 0 & 0 & 0 & 0 & 0 & 0 & 0 \\
0 & 0 & 0 & 0 & 0 & 0 & 0 & 0 & 0 & 0 & 0 & 0 & 0 & 0 \\
0 & 0 & \frac{13L}{35} & \frac{11L^2}{210} & \frac{-13L}{35} & \frac{-11L^2}{210} & 0 & 0 & \frac{9L}{70} & \frac{-13L^2}{420} & \frac{-9L}{70} & \frac{13L^2}{420} & 0 & 0 \\
0 & 0 & \frac{11L^2}{210} & \frac{L^3}{105} & \frac{-11L^2}{210} & \frac{-L^3}{105} & 0 & 0 & \frac{13L^2}{420} & \frac{-L^3}{140} & \frac{-13L^2}{420} & \frac{L^3}{140} & 0 & 0 \\
0 & 0 & \frac{-13L}{35} & \frac{-11L^2}{210} & \frac{13L}{35} & \frac{11L^2}{210} & 0 & 0 & \frac{-9L}{70} & \frac{13L^2}{420} & \frac{9L}{70} & \frac{-13L^2}{420} & 0 & 0 \\
0 & 0 & \frac{-11L^2}{210} & \frac{-L^3}{105} & \frac{11L^2}{210} & \frac{L^3}{105} & 0 & 0 & \frac{-13L^2}{420} & \frac{L^3}{140} & \frac{13L^2}{420} & \frac{-L^3}{140} & 0 & 0 \\
0 & 0 & 0 & 0 & 0 & 0 & 0 & 0 & 0 & 0 & 0 & 0 & 0 & 0 \\
0 & 0 & 0 & 0 & 0 & 0 & 0 & 0 & 0 & 0 & 0 & 0 & 0 & 0 \\
0 & 0 & \frac{9L}{70} & \frac{13L^2}{420} & \frac{-9L}{70} & \frac{-13L^2}{420} & 0 & 0 & \frac{13L}{35} & \frac{-11L^2}{210} & \frac{-13L}{35} & \frac{11L^2}{210} & 0 & 0 \\
0 & 0 & \frac{-13L^2}{420} & \frac{-L^3}{140} & \frac{13L^2}{420} & \frac{L^3}{140} & 0 & 0 & \frac{-11L^2}{210} & \frac{L^3}{105} & \frac{11L^2}{210} & \frac{-L^3}{105} & 0 & 0 \\
0 & 0 & \frac{-9L}{70} & \frac{-13L^2}{420} & \frac{9L}{70} & \frac{13L^2}{420} & 0 & 0 & \frac{-13L}{35} & \frac{11L^2}{210} & \frac{13L}{35} & \frac{-11L^2}{210} & 0 & 0 \\
0 & 0 & \frac{13L^2}{420} & \frac{L^3}{140} & \frac{-13L^2}{420} & \frac{-L^3}{140} & 0 & 0 & \frac{11L^2}{210} & \frac{-L^3}{105} & \frac{-11L^2}{210} & \frac{L^3}{105} & 0 & 0 \\
0 & 0 & 0 & 0 & 0 & 0 & 0 & 0 & 0 & 0 & 0 & 0 & 0 & 0 \\
0 & 0 & 0 & 0 & 0 & 0 & 0 & 0 & 0 & 0 & 0 & 0 & 0 & 0
\end{bmatrix} \tag{28}$$

where

E_{st}, E_c, and E_{rs}: modulus of elasticity of the steel beam, concrete, and slab reinforcement.

A_{st}, A_c, and A_{rs}: cross-sectional area of the steel beam, concrete slab, and slab reinforcement.

I_{st}: cross-section second moment of area of the steel beam element about its neutral axis.

L: beam element length.

I_c: cross-section second moment of area for the concrete slab element about its neutral axis.

d: distance from concrete slab neutral axis to slab reinforcement centroid.

K_s and K_n: connector layer element tangential and normal modulus (kN/mm^2).

CROSS-SECTION PROPERTIES

The modulus of elasticity for each material of the composite beam is a function of the strain value at the point under consideration. But the strains vary across the depth of the beam. This difficulty can be avoided by using the layered system. Steel beam section and concrete slab section are divided into a number of layers as shown in Fig. (4), so that:

$$EA = \int_A E dA = \sum_{il=1}^{n} E_{il} A_{il} \tag{29}$$

$$EI = \int_A E y^2 dA = \sum_{il=1}^{n} E_{il} y_{il}^2 A_{il} \tag{30}$$

where

n: the number of layers in the material under consideration.

E_{il}: the modulus of elasticity for the layer.

y_{il}: the distance from the layer center to the neutral axis of the concrete slab or the steel beam.

A_{il}: the cross-sectional area of the layer.

In an incremental nonlinear analysis, the values of the tangential modulus, K_s, and normal modulus, K_n, of the shear connector layer, the elastic modulus of the concrete slab reinforcement, E_{rs}, steel beam modulus of elasticity, E_{st}, and concrete slab modulus of elasticity, E_c, are obtained from the corresponding constitutive relationships (Figs. (5) to (8)) by replacing them with the corresponding tangent moduli.

CALCULATION OF INTERNAL RESISTING FORCES

The internal resisting forces have to be evaluated as accurate as possible for the unbalanced force iteration procedure (Frodin et al., 1978). Thus, these forces are evaluated using three Gaussian quadrature points along the length of the element combined with layer integration for steel beam and concrete slab sections, as follows (Chapman, 1964):

$$\{F_i\} = \int_{vol} [B]^T \{\sigma\} dvol = \sum_{P=1}^{3} w_p \{\bar{\sigma}\}_P |J| \tag{31}$$

and integration across the depth of the sections:

$$\{\bar{\sigma}\}_P = \int_{c1}^{c2} [B]_P \{\sigma\}_P dA = \sum_{il=1}^{n} [B_{il}]_P \{\sigma_{il}\} A_{il} \tag{32}$$

Then,

$$\{F_i\} = \sum_{P=1}^{3} w_P \sum_{il=1}^{n} [B_{il}]_P \{\sigma_{il}\}_P A_{il} |J| \tag{33}$$

where

c_1 and c_2: the top and bottom layers of the section.

$|J|$: the determinant of the Jacobian matrix of the transformation and it is equal to L/2.

P : the Gaussian integration points (-0.77459667, 0.0, 0.77459667).

w_P : the weight of integration of the Gaussian quadriture points (0.555555, 0.888888, 0.555555).

The shear connector properties are:

$$\left.\begin{aligned} K_s &= \frac{N_{co.}K_s}{P} \quad (kN/mm^2) \\ q_u &= \frac{N_{co.}Q_u}{P} \quad (kN/mm) \\ .K_n &= \frac{N_{co.}K_n}{P} \quad (kN/mm^2) \\ k_n &= \frac{E_{co.}A_{co.}}{L_{co.}} \quad (kN/mm).....in\ tension\ (separation). \\ k_n &= \frac{4G_c r_c}{(1-\mu_c)} \quad (kN/mm)\ [30].....in\ compression\ (contact) \end{aligned}\right\} \qquad (34)$$

where

Q_u : ultimate capacity of one connector (kN),

q_u : ultimate capacity of equivalent connector layer (kN/mm),

$N_{co.}$: No. of shear connectors in the cross-section,

P : longitudinal spacing of connectors,

K_s : tangential modulus of shear connector layer (kN/mm^2),

k_s : tangential stiffness of shear connector layer (kN/mm),

K_n : normal modulus of shear connector layer (kN/mm^2),

k_n : normal stiffness of shear connector layer (kN/mm),

$E_{co.}$: Young's modulus of stud connector material,

$A_{co.}$ and $L_{co.}$: the cross-sectional area and the length of the stud shank, respectively,

G_c : modulus of rigidity of the concrete,

r_c : radius of equivalent concrete plate,

μ_c : Poisson's ratio of concrete.

CONVERGENCE CRITERIA

The force criterion is based on a comparison between the unbalanced and external loads, and this is defined as (Owen and Hinton, 1980):

$$\frac{\sqrt{\left[\sum_{i=1}^{N}(F_u^t)_i^2\right]}}{\sqrt{\left[\sum_{i=1}^{N}(F_j)_i^2\right]}} \times 100 \le TOLER \qquad (35)$$

where N is the number of total degrees of freedom in the problem and t denotes the iteration number.

This criterion states that convergence occurs if the norm of unbalanced forces becomes less than TOLER times the norm of the total applied force.

NORMAL MODULUS OF SHEAR CONNECTORS

When the load is applied on the composite beam, regions of negative uplift (compression between concrete slab and steel beam) and positive uplift (separation between concrete slab and steel beam)

will be developed. The normal stiffness of shear connector layer k_n, in negative uplift differs from that for positive uplift. The difficulty appears in specifying the regions of negative and positive uplift.

A special technique is adopted in the computer programs. The solution begins with equal values of normal stiffness of shear connector layer k_n, for positive and negative uplift regions. The values of uplift are calculated. From which, regions of negative and positive uplift are specified. Then, the solution is repeated with different values of normal stiffness of shear connector layer k_n, according to the regions of positive and negative uplift. This procedure is continued until convergence in the length of regions of negative and positive uplift is achieved.

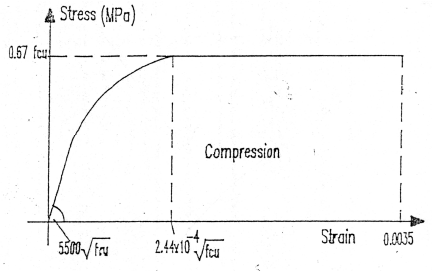

Fig. (5) BS 8110 compressive stress-strain curve for concrete.

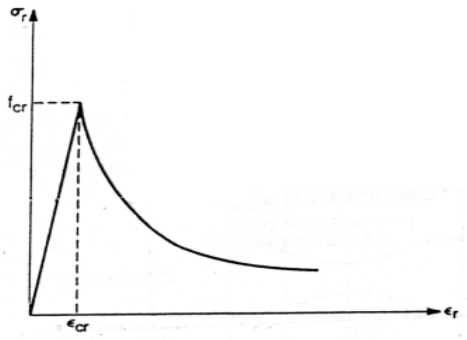

Fig. (6) Mathematical model for concrete tension softening.

ANALYSIS OF COMPOSITE BEAMS

The efficiency of the present work is demonstrated by the use of the computer program (QHA2) (Al-Aquly, 2002), which analyzes the composite beam as a one-dimensional problem, is assessed by comparing with the experimental results obtained from previous researchers. Also, a comparison with the two- and three-dimensional analysis using the program (MHND) and the software (ANSYS 5.4), respectively is shown.

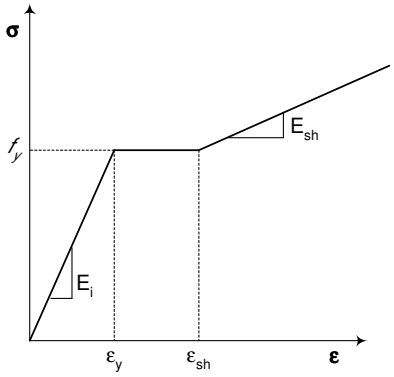

Fig. (7) Idealized stress-strain curve for steel.

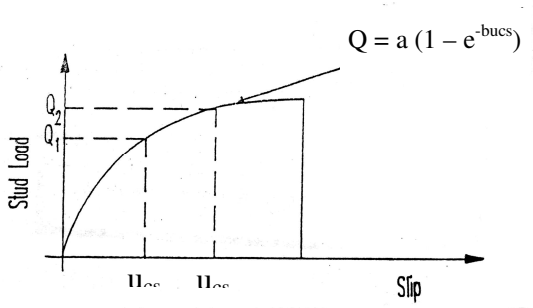

Fig. (8) Load-slip relationship for shear connectors.

Teraskiewicz Composite Beam

Teraskiewicz (1967) tested a two-span continuous composite beam of 6.7m long and under two-point loading. Fig. (9) shows the beam geometry, cross-section dimensions and load setup. The material properties of the composite beam are shown in **Table (1).**

Fig. (10) shows the deflected shape of the beam as predicted from the linear analysis

compared with the experimental results. It can be seen that the present study gives results in good agreement with the experimental values.

Table (1) Material properties of composite beam tested by Teraskiewicz (1967).

Material	Properties
Steel beam	Yield stress = 285 MPa Young's modulus = 200000 MPa Strain hardening modulus = 1000 MPa ν = 0.3
Concrete	$f_c^{'}$ = 48 MPa Young's modulus = 27600 MPa ν = 0.15 f_{cr} = 4.8 MPa
Reinforcement	Yield stress = 310 MPa Young's modulus = 200000 MPa ν = 0.3 Top transverse = ϕ 8 @ 102 mm C/C Top longitudinal = ϕ 8 @ 65 mm C/C Bottom transverse = ϕ 4.8 @ 204 mm C/C Bottom longitudinal = ϕ 8 @ 204 mm C/C
Shear stud connector	Spacing = 146 mm Diameter x height = 9x50 mm Number of rows = 2

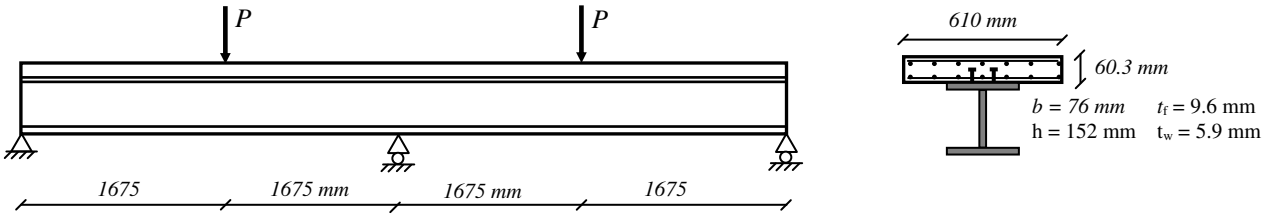

Fig. (9) Composite continuous beam tested by Teraskiewiez (1967).

Due to partial interaction, slip always takes place between concrete slab and steel beam. Slip distribution for composite beam is shown in Fig. (11). A comparison is made with the experimental results and a good correlation is obtained. For the purpose of the current analysis the shear force-slip relationship proposed by Yam and Chapman (1968 and 1972) is used.

$$Q = 32\,(1 - e^{-4.75 u_{cs}}) \qquad (36)$$

where Q is the shear force in kN, and u_{cs} is the slip in mm.

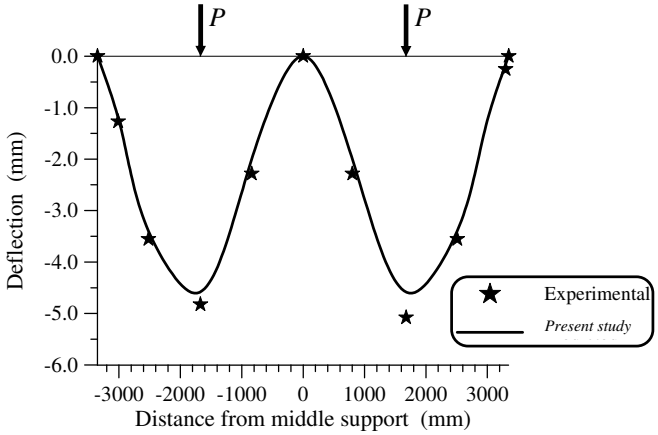

Fig. (10) Deflected shape of Teraskiewiez composite beam at load P = 57 kN.

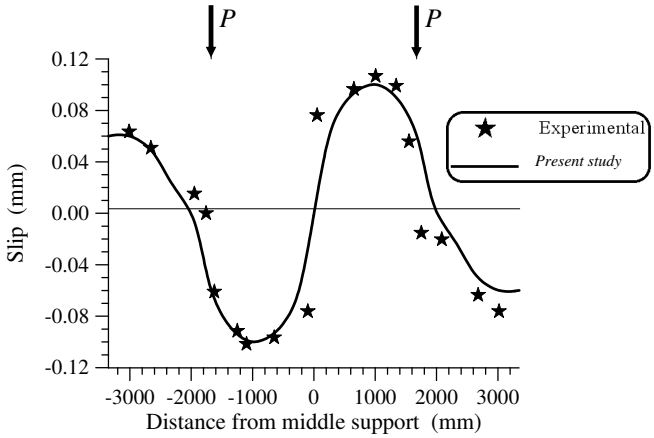

Fig. (11) Slip distribution of Teraskiewiez composite beam at load P = 57 kN.

Due to symmetry, both in geometry and loading in this continuous composite beam, only half of the beam is idealized by introducing the appropriate boundary conditions along the beam centerline.

The discretization of the beam in finite element method is investigated. The composite beam is divided into 10, 15, and 20 elements. The deflected shape along half the beam span is shown in **Fig. (12).** It is found that the deflection values when using 15 or 20 elements are approximately equal, so that the use of 15 elements seems to be sufficient.

In this analysis, using the one-dimensional finite element program developed in this study (QHA2), the beam was divided into 15 elements while the cross-section was divided into 15 layers of concrete and 16 layers of steel (4 layers for each flange and 8 layers for the web of steel beam).

Fig. (13) illustrates the two-dimensional finite element representation mesh for the beam. Concrete slab and steel beam are idealized by using 138 and 322 four-noded plane stress elements, respectively. Reinforcement is idealized by 92 truss bar elements. 186 bond-slip linkage elements of zero length are used to represent the bond-slip between concrete and reinforcement. The interface between the concrete slab and steel beam is idealized by 47 shear-friction interface elements. Shear connectors are idealized by 23 stub connector elements. The total number of nodes resulting from the above idealization is 750 nodes.

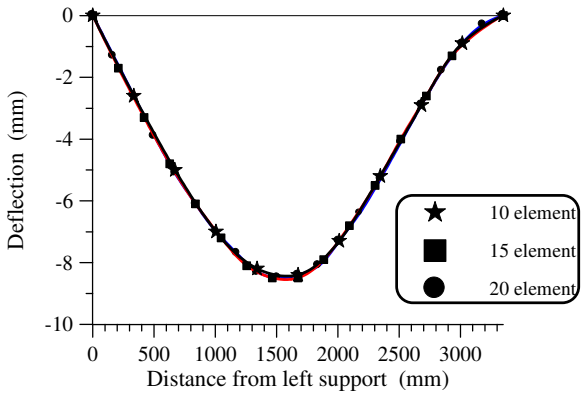

Fig. (12) The deflected shape along half the beam span.

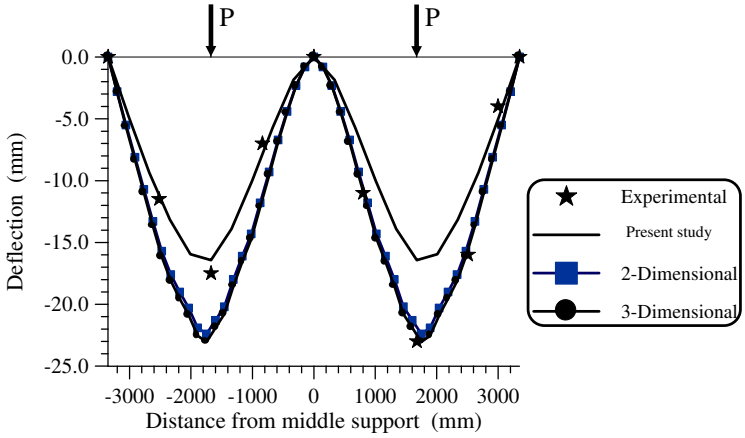

Fig. (15) Deflected shape of Teraskiewicz composite beam at load P = 122 kN.

The three-dimensional finite element representation mesh for the whole beam (ignore symmetry) using the (ANSYS 5.4) software is shown in **Fig. (14).** Concrete slab is idealized by using 3312 eight-noded brick elements (Solid 65 - reinforced concrete element), and steel beam is idealized by using 1012 four-noded shell elements (Shell 43 - plastic shell). Reinforcement is imbedded in the concrete brick elements. The interface between the concrete slab and steel beam is idealized by 465 two-noded contact elements (Contact 52 – point to point contact). Shear connectors are idealized by 92 two-noded nonlinear spring (Combine 39) to resist slip and 92 two-noded linear spring (Combine 40) to resist uplift separation. The total number of nodes resulting from the above idealization is 5952 nodes.

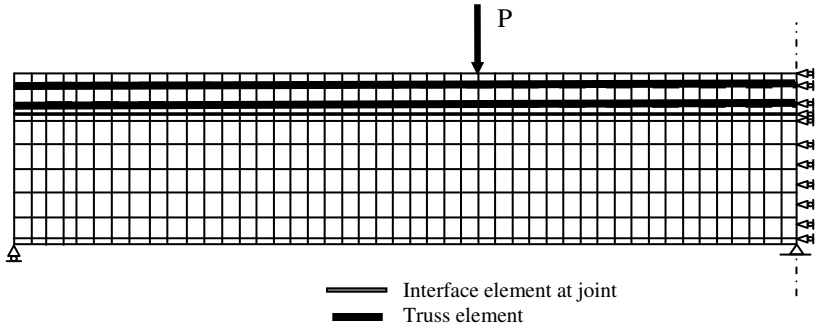

Fig.(13) Two-dimensional finite element discretization of continuos composite beam tested by Teraskiewicz (1967).

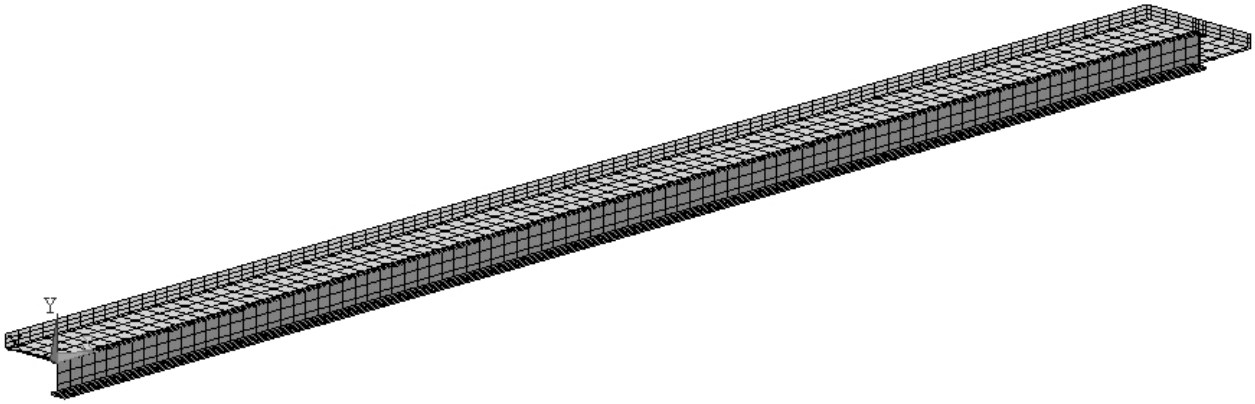

Fig. (14) Three-dimensional finite element discretization of continuos composite beam tested by Teraskiewicz (1967).

An incremental load is applied on concrete slab at its proper position. The number of increments depends on the program used, and ranges between 50 and 70 increments.

Fig (15) compares measured and predicted deflected shape of Teraskiewicz composite beam at load P = 122 kN (87% of the predicted ultimate load). Up to this load level, the analysis had predicted extensive yielding of the steel beam, together with significant cracking of the concrete and some yielding of the reinforcement over the central support. The good agreement demonstrates the reliability of the suggested representation well into the elastoplastic range of loading.

Fig(16) shows a comparison in the load mid-span deflection curve of the composite beam, using the three methods of representation. It can be seen that the proposed method seems a little stiffer than the other representations.

The slip distribution along the beam axis at load P = 122 kN is shown in Fig. (17). The computed slips show good agreement with the measured response on the left side of the beam centerline. The results on the right side do not compare as well. This is due to the normal variations encountered in experimental work. Since in this analysis symmetry is assumed, such anomalies cannot be accounted for. The curves show that the maximum slip is located about 1000 mm from the mid-support.

The general form of the slip distribution is in keeping with that expected from the shear force diagram, with the added effect of shear connector flexibility giving rise to a smoothing out of the slip diagram near the support and load point.

In computer analysis, a limiting value of slip capacity must be assumed. Since this could not be directly measured during the beam test, the following method was used. In this method the curve of load against measured maximum slip was plotted. By extrapolation, the maximum slip corresponding to the failure load was found to be 1.25 mm. This was then taken as the limiting of the shear connection.

Uplift movement (normal separation) distribution in the interface between the concrete slab and steel beam of the Teraskiewicz continuous composite beam is shown in Fig. (18). It indicates that there are regions of positive uplift (separation) and negative uplift (compression) at the interface of concrete slab and steel beam.

Stress distribution in the top reinforcement along the Teraskiewicz composite beam axis at load P = 122 kN is shown in **Fig. (19)**. This distribution indicates that the maximum compressive stress is about 1800 mm from the mid-support and that the tension region is not more than 800 mm at each side of the mid-support.

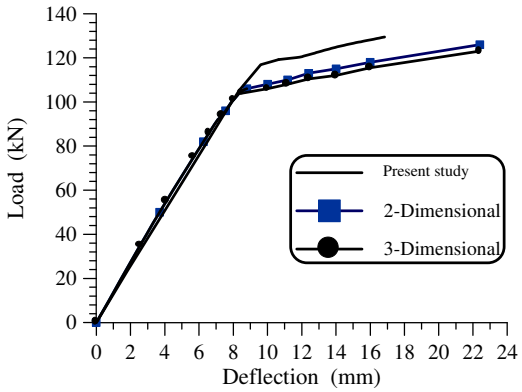

Fig. (16) Load mid-span deflection of Teraskiewicz composite beam.

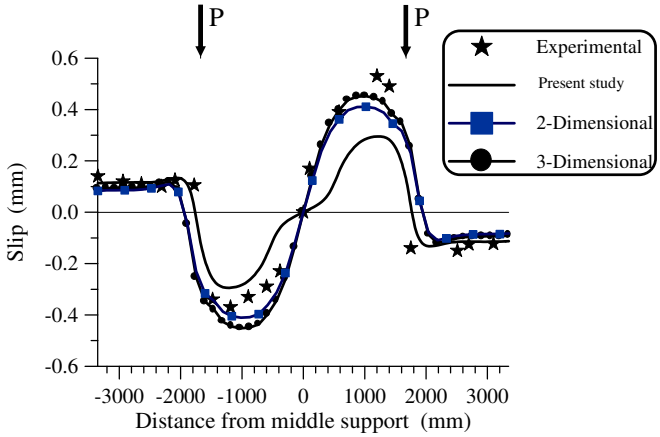

Fig. (17) Slip distribution along the Teraskiewicz composite beam axis at load P = 122 kN.

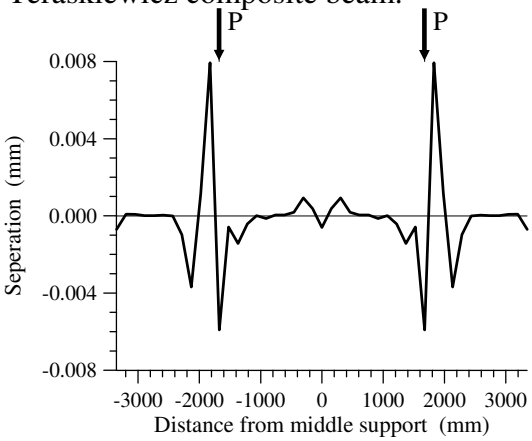

Fig. (18) Uplift movement distribution along the Teraskiewiez composite beam axis at load P = 122 kN.

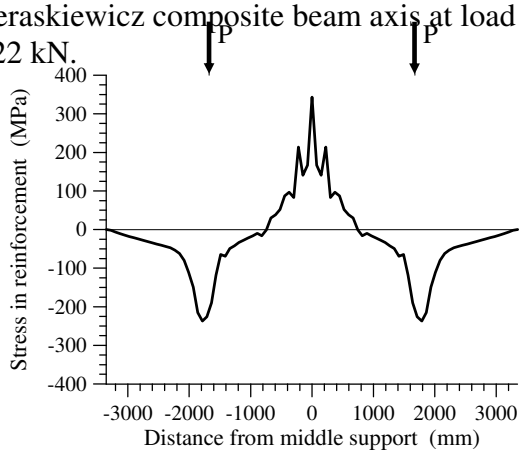

Fig. (19) Stress in top reinforcement distribution along the Teraskiewicz composite beam axis at load P = 122 kN.

An ultimate load of 151 kN was obtained during the actual test, at which stage shear connector failure was observed in the region between the central supports and the left hand mid span, the present study predicted an ultimate load of 140 kN with the predicted mode of failure involving failure of the shear connectors within the same region as was observed in the experiments. The predicted progression of yielding through the I-section steel beam is seen that the yielded regions within the inner half of the span remain confined, even at ultimate loading. This is due to the very high moment gradient within inner half span, causing flexural effects to drop off very sharply at small distances away from locations of maximum moment.

Ansourian Composite Beams

Ansourian (1981) tested a series of two-span continuous composite steel-concrete beams, details of two of them (CTB1 and CTB2) are shown in Fig. (20). Material properties of these two beams are listed in Table (2).

Table (2) Material properties of composite beams (CTB1 and CTB2) tested by Ansourian (1981).

Material	Properties
Steel beam	Yield stress = 308.5 MPa Young's modulus = 200000 MPa Strain hardening modulus = 5000 MPa $\nu = 0.3$
Concrete	f_{cu} = 30 MPa (CTB1); 50 MPa (CTB2) $\nu = 0.15$
Reinforcement	Yield stress = 430 MPa Young's modulus = 200000 MPa $\nu = 0.3$ Hog top = 800 mm^2 (CTB1); 1230 mm^2 (CTB2) Hog bottom = 316 mm^2 (CTB1); 470 mm^2 (CTB2) Sag top = 360 mm^2 (CTB2) Sag bottom = 160 mm^2 (CTB1 & CTB2)
Shear stud connector	Spacing = 273 mm Diameter x height = 19x75 mm Number of rows = 2

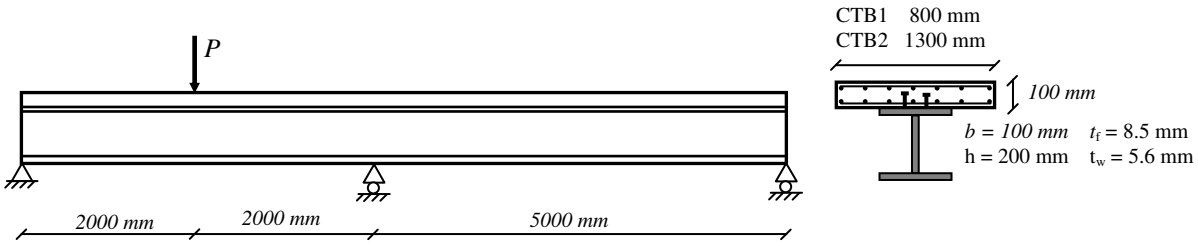

Fig. (20) Composite continuous beams tested by Ansourian (1981).

Using the finite element program (QHA2), Ansourian composite beam (CTB1) was divided into 36 elements while the cross-section was divided into 15 layers of concrete and 16 layers of steel (4 layers for each flange and 8 layers for the web of steel beam).

Fig. (21) represents the load mid-spans (left and right) deflection curve of the composite beam (CTB1). The same trend of behavior is seen for the numerical and the test results, but comparison with experimental results indicates a close agreement till about 85% of the ultimate load. A stiffer behavior of the finite element models was observed during the next load increments. This may be attributed to the selfweight effects on the stresses and strains, which were neglected in the analysis. However, the analytical ultimate load level (198 kN) is detected quite well compared with the experimentally observed of 201 kN, with an error of only 1.5%.

Steel strains at lower flange of Ansourian composite beam (CTB1) at both critical sections (below the load and above mid-support) are shown in Fig. (22). At the last few increments of loading, the strain at the sagging section increased rapidly from 0.008 to 0.016.

Comparison between experimental and predicted results in mid-spans deflection and steel strains at lower flange for the composite beam (CTB2) are shown in Figs. (23) and (24), respectively.

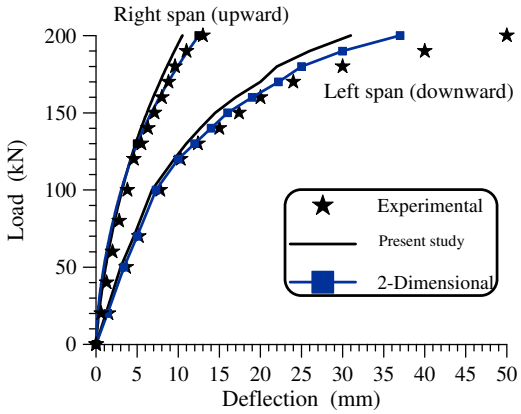

Fig. (21) Load mid-span deflection of Ansourian composite beam (CTB1).

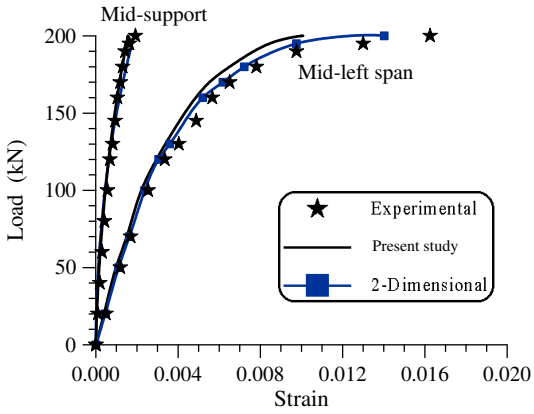

Fig. (22) Steel strain at lower flange of Ansourian composite beam (CTB1).

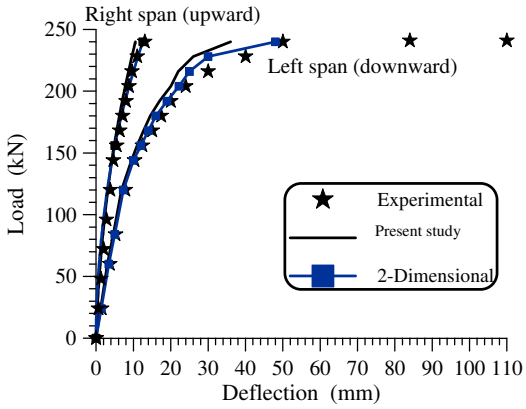

Fig. (23) Load mid-span deflection of Ansourian composite beam (CTB2).

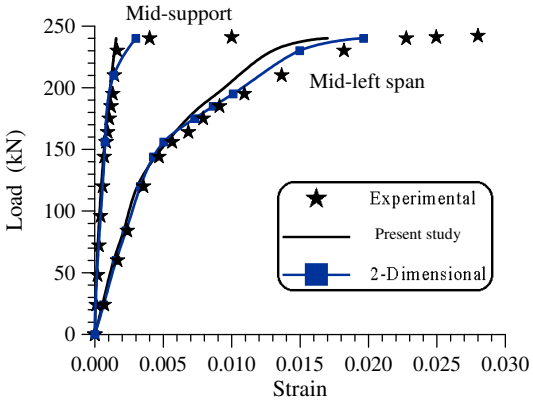

Fig. (24) Steel strain at lower flange of Ansourian composite beam (CTB2).

CONCLUSIONS

Based on the results obtained from this investigation, the followings can be concluded:
-The proposed method of the finite element analysis with the developed composite beam element appears to be valid and powerful for both linear and nonlinear analysis of composite beams.
-The adopted material constitutive relationships are found to give satisfactory results at both the surface and ultimate load stages.
-The two horizontal degrees of freedom that are used at mid-length of the element improve its behavior to predict the slip; these degrees of freedom have no direct effect on the flexural behavior of the element.
Using the layered approach and the incremental iterative solution procedure, the proposed nonlinear finite element model can incorporate any realistic relationship for the constituent materials, which make up the beam.

REFERENCES

Al-Aquly, Qusay A., 2002 “Analysis of Continuous Composite Concrete-Steel Girders with Partial Interaction.”, M.Sc. Thesis, University of Baghdad, 2002, 140pp.

Al-Sherrawi, Mohannad H., 2000 "Shear and Moment Behavior of Composite Concrete Beams", Ph.D. Thesis, University of Baghdad, Iraq, 2000,135pp.

Ansourian, P., 1981 "Experiments on Continuous Composite Beams", Proceedings of the Institution of Civil Engineers, Part 2, Vol.71, December 1981, pp. 25-51.

British Standards Institution, BS8110, 1985: Structural Use of Concrete: Part 1. Code of Practice for Design and Construction: Part 2. Code of Practice for Special Circumstances, British Standards Institution, London, 1985.

Chapman, J. C., 1964 "Composite Construction in Steel and Concrete-The Behavior of Composite Beams", Journal of the Structural Engineer, Vol.42, No.4, April 1964, pp. 115-125.

Frodin, J. G., Taylor, R. and Stark, J. W., 1978 "A Comparison of the Deflections in Composite Beams having Full and Partial Shear Connection", Proceedings of the Institution of Civil Engineers, Part 2, Vol.65, June 1978, pp. 307-322.

Hamad, N. T., 2000 "Nonlinear Analysis of Continuous Composite Beams with Partial Connection", M.Sc. Thesis, Al-Mustansiriya University, Iraq, 2000.105pp.

Owen, D. R. J. and Hinton, E., 1980 “Finite Element in Plasticity: Theory and Practice,” Pineridge Press Limited, Swansea, U.K., 1980, 329 pp.

Teraszkiewicz, J. S., 1967 "Static and Fatigue Behavior of Simply Supported End Continuous Beams of Steel and Concrete", Ph.D. Thesis, London University, 1967 (cited according to Hamad, 2000).

Yam, L. C. P. and Chapman, J. C., 1972 "The Inelastic Behavior of Continuous Composite Beams of Steel and Concrete", Proceedings Institution of Civil Engineers, Part 2, Vol.53, December 1972, pp. 487-501.

Yam, L. C. P. and Chapman, J. C., 1968 "The Inelastic Behavior of Simply Supported Composite Beams of Steel and Concrete", Proceedings Institution of Civil Engineers, Part 2, Vol.41, December 1968, pp. 651-683.

NOTATIONS

A_{il} : the cross-sectional area of the layer.

A_{st}, A_c, and A_{rs} : cross-sectional area of the steel beam, concrete slab, and slab reinforcement.

$A_{co.}$ and $L_{co.}$: the cross-sectional area and the length of the stud shank, respectively.

c_2 : the top and bottom layers of the section.

d : distance from concrete slab neutral axis to slab reinforcement centroid.

E_{il} : the modulus of elasticity for the layer.

E_{st}, E_c, and E_{rs} : modulus of elasticity of the steel beam, concrete, and slab reinforcement.

$E_{co.}$: Young's modulus of stud connector material.

G_c : modulus of rigidity of the concrete,

I_c : cross-section second moment of area for the concrete slab element about its neutral axis.

I_{st} : cross-section second moment of area of the steel beam element about its neutral axis.

$|J|$: the determinant of the Jacobian matrix of the transformation and it is equal to L/2.

$[k^e]_{st}$, $[k^e]_c$, $[k^e]_{rs}$, $[k^e]_{cs}$, and $[k^e]_{sc}$: steel beam, concrete slab, tangential shear connector layer, and transverse shear connector layer element stiffness matrix.

k_n : normal stiffness of shear connector layer (kN/mm).

$[k_o]$: the stiffness matrix of the composite beam without shear interaction,

K_s and K_n : connector layer element tangential and normal modulus (kN/mm^2).

k_s : tangential stiffness of shear connector layer (kN/mm).

$[k_{slip}]$ and $[k_{uplift}]$: shear connector contribution to the beam stiffness.

L : beam element length.

N is the number of total degrees of freedom in the problem

n : the number of layers in the material under consideration.

$N_{co.}$: No. of shear connectors in the cross-section.

P : longitudinal spacing of connectors.

P : the Gaussian integration points (-0.77459667, 0.0, 0.77459667).

Q : the shear force in kN, and u_{cs} is the slip in mm.

Q_u : ultimate capacity of one connector (kN).

q_u : ultimate capacity of equivalent connector layer (kN/mm).

r_c : radius of equivalent concrete plate.

t: denotes the iteration number.

$u_{0st}(x)$ and $u_{0c}(x)$: the axial displacements of the steel beam and of the concrete slab respectively.

w_P : the weight of integration of the Gaussian quadriture points (0.555555, 0.888888, 0.555555).

$w_{st}(x)$ and : $w_c(x)$ the vertical displacements for the steel beam and the concrete slab, respectively.

y_{il} : the distance from the layer center to the neutral axis of the concrete slab or the steel beam.

y_{st} and y_c : the distances from the reference points to the interface of the steel and concrete components.

ε_{0st} and ε_{0c} are the axial strains at the reference axes of the steel and the concrete sections, respectively.

ν : Poisson's ratio.

$\theta_{st} = \frac{dw_{st}}{dx}$ and $\theta_c = \frac{dw_c}{dx}$: the slopes of the steel and concrete components.